Journal of Power Sources 300 (2015) 438–443

Contents lists available at ScienceDirect

Journal of Power Sources

journal homepage: www.elsevier.com/locate/jpowsour

A comparative study of all-vanadium and iron-chromium redox flow batteries for large-scale energy storage

Y.K. Zeng, T.S. Zhao*, L. An, X.L. Zhou, L. Wei

Department of Mechanical and Aerospace Engineering, The Hong Kong University of Science and Technology, Clear Water Bay, Kowloon, Hong Kong Special Administrative Region

HIGHLIGHTS

- Performance and cost of the VRFB and ICRFB are compared.
- Energy efficiencies of the VRFB and ICRFB are similar at high current densities.
- The ICRFB exhibits a higher capacity decay rate than does the VRFB.
- The ICRFB shows cost advantages at high power densities and large capacities.

ARTICLE INFO

Article history:
Received 16 August 2015
Received in revised form
10 September 2015
Accepted 26 September 2015
Available online xxx

Keywords:
Comparative study
Vanadium redox flow battery
Iron-chromium redox flow battery
Large-scale energy storage
Capital cost

ABSTRACT

The promise of redox flow batteries (RFBs) utilizing soluble redox couples, such as all vanadium ions as well as iron and chromium ions, is becoming increasingly recognized for large-scale energy storage of renewables such as wind and solar, owing to their unique advantages including scalability, intrinsic safety, and long cycle life. An ongoing question associated with these two RFBs is determining whether the vanadium redox flow battery (VRFB) or iron-chromium redox flow battery (ICRFB) is more suitable and competitive for large-scale energy storage. To address this concern, a comparative study has been conducted for the two types of battery based on their charge–discharge performance, cycle performance, and capital cost. It is found that: i) the two batteries have similar energy efficiencies at high current densities; ii) the ICRFB exhibits a higher capacity decay rate than does the VRFB; and iii) the ICRFB is much less expensive in capital costs when operated at high power densities or at large capacities.

1. Introduction

Renewable energy sources such as wind and solar energy have gained increasing attention due to growing environmental issues and sustainability over fossil fuel consumption. These renewables are intermittent and fluctuant in nature, requiring the need of large-scale energy storage systems for continuous and reliable power output. Redox flow batteries (RFBs) are electrochemical devices that utilize the electrochemical reactions between two redox couples to reversibly conduct the conversion between chemical energy and electrical energy. As shown in Fig. 1, an RFB consists of two flowing electrolyte solutions (positive and negative electrolytes) and two electrodes separated by an ion-exchange membrane (or a separator). The soluble reactants are contained within separate storage tanks and pumped through the porous electrodes where the electrochemical reactions (reduction and oxidation) take place. RFBs have several unique advantages including scalability, high energy efficiency, fast response, intrinsic safety, and long lifetime [1–3].

The iron chromium redox flow battery (ICRFB) is considered as the first true RFB and utilizes low-cost, abundant chromium and iron chlorides as redox-active materials, making it one of the most cost-effective energy storage systems [2,4]. The ICRFB typically employs carbon felt as the electrode material, and uses an ion-exchange membrane to separate the two electrodes. The ICRFB produces a standard voltage of 1.18 V through the following reactions:

Positive electrode:

$$Fe^{3+} + e^{-} \underset{charge}{\overset{discharge}{\rightleftharpoons}} Fe^{2+} \quad E^{0} = +0.77\ \text{V vs. SHE} \tag{1}$$

* Corresponding author.
E-mail address: metzhao@ust.hk (T.S. Zhao).

http://dx.doi.org/10.1016/j.jpowsour.2015.09.100
0378-7753/

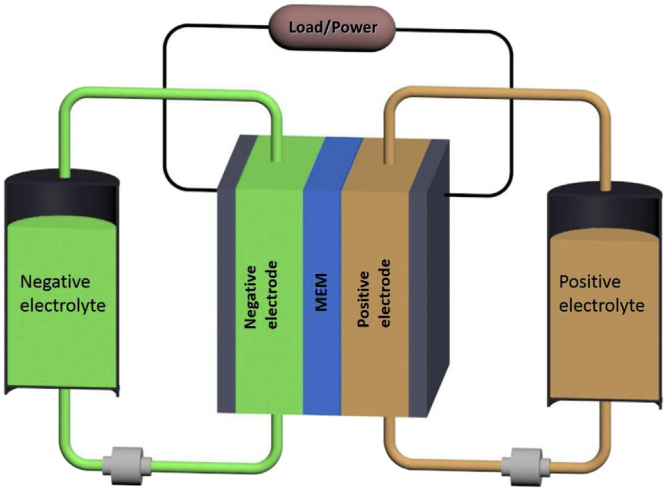

Fig. 1. Schematic of a redox flow battery.

Negative electrode:

$$Cr^{2+} \underset{charge}{\overset{discharge}{\rightleftharpoons}} Cr^{3+} + e^- \quad E^0 = -0.41\ \text{V vs. SHE} \tag{2}$$

Overall:

$$Fe^{3+} + Cr^{2+} \underset{charge}{\overset{discharge}{\rightleftharpoons}} Fe^{2+} + Cr^{3+} \quad E^0 = 1.18\ \text{V} \tag{3}$$

Extensive studies on ICRFBs have been carried out over the past few decades [5–8]. Due to the fast kinetics of the Fe(II)/Fe(III) redox reaction, bare carbon felt is typically adopted as the electrode material at the positive side, while at the negative side, the catalyst is generally necessary to enhance the electrochemical kinetics of the Cr(II)/Cr(III) redox reaction. Meanwhile, the catalyst must have a high overpotential towards the hydrogen evolution reaction because thermodynamically, hydrogen ions are more easily reduced than Cr(III) ions. Hydrogen evolution not only reduces the coulombic efficiency, but also causes the state of charge (SOC) of positive and negative electrolytes to be imbalanced over prolonged cycles, eventually causing capacity decay. To counter these issues, catalysts, such as Bi and Au–Tl, are deposited on the electrode surface to enhance the electrochemical kinetics of the Cr(II)/Cr(III) redox reaction, and alleviate hydrogen evolution [5,8]. In addition, a rebalance cell that manages produced hydrogen and rebalances the SOC of electrolytes can be installed to avoid the negative effects of hydrogen evolution on the battery capacity [9].

Another problem is that membranes in ICRFBs are permeable not only to charge-carrier ions (H^+/Cl^-), but also to active species (Fe and Cr ions). On the other hand, the use of Fe and Cr ions on the positive and negative electrodes, respectively, creates a large concentration difference through the membrane for the respective ions, resulting in a high crossover rate and serious capacity decay even after short-term operation. To tackle this issue, the mixed-reactant solutions consisting of premixed Fe and Cr salts were proposed for both positive and negative electrolytes, which significantly reduced the net crossover rates, thereby enabling lengthier operation [10]. Although the incorporation of mixed-reactants shows promise, long-term operation of ICFB still leads to some redox-ion crossover caused by electro-migration, diffusion and convection. The capacity decay in during long-term operation can be somewhat recovered by simply remixing the positive and negative electrolytes, which is typically executed in redox flow batteries [9,11,12]. In addition to the fundamental research, extensive efforts have been made to scale-up the ICRFB for the purpose of large-scale energy storage [9,13–16]. For instance, a 250 kW/1 MWh ICRFB energy storage system has been demonstrated in California, the US [16].

Radically different from the ICRFB, the vanadium redox flow battery (VRFB) that utilizes V(II)/V(III) and V(IV)/V(V) redox couples eliminates cross-contamination between negative and positive compartments [17]. In addition, the VRFB has particular advantages, such as excellent electrochemical kinetics and negligible side reaction [18–20]. In VRFBs, the electrochemical reactions are as follows:

Positive electrode:

$$VO_2^+ + 2H^+ + e^- \underset{charge}{\overset{discharge}{\rightleftharpoons}} VO^{2+} + H_2O \quad E^0 = +1.01\ \text{V vs. SHE} \tag{5}$$

Negative electrode:

$$V^{2+} \underset{charge}{\overset{discharge}{\rightleftharpoons}} V^{3+} + e^- \quad E^0 = -0.25\ \text{V vs. SHE} \tag{6}$$

Overall:

$$VO_2^+ + V^{2+} + 2H^+ \underset{charge}{\overset{discharge}{\rightleftharpoons}} VO^{2+} + V^{3+} + H_2O \quad E^0 = 1.26\ \text{V} \tag{7}$$

The VRFB was invented and pioneered by Skyllas-Kazacos and co-workers at the University of New South Wales in the 1980s [17,21]. In the past few decades, much effort has been focused on further improving the battery performance, such as fabricating powerful catalysts, optimizing electrodes and membranes, and developing numerical tools [22–29]. However, market penetration of the VRFB for large-scale energy storage is limited by the high capital cost, which results from the use of expensive vanadium redox couples [11,19] and Nafion membranes. It is shown that a VRFB system with a 4-h discharge duration has an estimated capital cost of \$447 kWh^{-1}, in which the electrolyte and membrane account for 43% and 27%, respectively [30]. However, the targeted capital cost for a large-scale energy storage system is estimated to be at \$100 kWh^{-1} [31]. Reducing the capital cost remains a major challenge for the commercialization of VRFBs.

In summary, the ICRFB uses low-cost redox-active materials, but suffers from system complexity due to the need for SOC rebalancing. While the VRFB exhibits excellent kinetics, it is off-set by its high capital cost. The above discussion between VRFBs and ICRFBs raises an open-ended question: which technology is more competitive for large-scale energy storage systems? The objective of this work is to attempt to answer this question via conducting a comparative study in terms of the charge–discharge performance, cycle performance, and capital cost. The energy efficiency and capacity decay rate of the VRFB and ICRFB are examined from the experiments. An analysis of the capital cost was conducted based on these obtained figures.

2. Experimental

A typical flow-through cell structure was adopted for the battery tests. Both negative and positive electrodes were composed of 2.0 cm × 2.5 cm active area (SGL, GFA 6) graphite felt. The electrodes were treated at 400 °C for 6 h in ambient air to enhance the electrochemical activity and hydrophilicity [32]. Silica gaskets were selected to give a compression ratio of 20% for both the negative and positive electrodes. Nafion 212 is used for the membrane.

20 mL solutions of 1.0 M $VOSO_4$ (ZhongTian Chemical Ltd. China) + 3.0 M H_2SO_4 (Sigma–Aldrich) and 1.0 M V(III) + 3.0 M H_2SO_4 were used as the positive and negative electrolytes, respectively for the VRFB. 20 mL mixed solutions of 1.0 M $FeCl_2$ (Aladdin) + 1.0 M $CrCl_3$ (Aladdin) + 3.0 M HCl (Sigma–Aldrich) + 0.01 M Bi^{3+} (Bi_2O_3: Aladdin) were used as both negative and positive electrolytes for the ICRFB. The electrolytes were circulated at a flow rate of 50 mL min^{-1} using a 2-channel peristaltic pump (WT-600-2J, Longer pump, China). The charge–discharge tests and cycle tests were conducted using Arbin BT2000 (Arbin® Instrument). The cell and the electrolyte reservoir were kept in a temperature chamber at a designated temperature. The VRFB was charged and discharged at 40, 80, 120, 160 mA cm^{-2} with cutoff voltage between 1.0 and 1.6 V under room temperature (25 °C), and the cycle test was conducted at 80 mA cm^{-2}. Meanwhile, ICRFB was charged and discharged at 40, 80, 120, 160 mA cm^{-2} with cut-off voltage between 0.8 and 1.2 V at 65 °C, and its cycle test was conducted at 80 mA cm^{-2}.

3. Capital cost analysis

For the flow battery design, the power and energy requirements determine the size of the cell stacks and the amount of electrolyte, respectively. The cost of RFBs is determined by the power and energy part, which can be estimated as follows [33]:

$$A = \frac{P_{rated} + P_{loss}}{i_d \overline{V}_d} \tag{8}$$

$$V = \frac{2t_d(P_{rated} + P_{loss})}{\varepsilon \overline{V}_d x F} \tag{9}$$

$$C_p = A\sum_i C_{P,i} + C_{P,M} \tag{10}$$

$$C_E = \frac{(P_{rated} + P_{loss})t_d\left(\sum_i Q_i M_i S_i\right)}{\varepsilon n F \overline{V}_d} + C_{E,M} + Q_t V \tag{11}$$

$$C_T = C_P + C_E + C_{BOP} \tag{12}$$

The component cost data listed in Table 3 are referenced from the open literature [19,30,34] and various websites [35]. The VRFB and ICRFB electrolytes are calculated based on V_2O_5 and ferrochomium, respectively. The chromium content in ferrochomium is 71.4% [35], and any extra iron required is derived from iron scrap. The system loss of the two batteries, including pump loss and shunt current loss is assumed to be the same for the sake of simplicity. For the ICRFB, the iron–chlorine electrolysis cell is selected as the rebalancing cell due to its excellent stability, and one rebalancing cell is installed for every 100-cell stack. The amount of evolved hydrogen is around 1% of charge capacity per cycle [10], and the voltage for the iron-chlorine rebalance cell is 0.6–0.8 V [9]. Therefore, 1% energy efficiency loss is estimated for the rebalancing process. To offset the extra loss caused by rebalancing and achieve the same system energy efficiency as the VRFB, the current density of the ICRFB needs to be decreased to achieve higher energy efficiency of the single cell, which will lead to larger cell stacks for the given power requirement and increase the capital cost. The current density of the VRFB at energy efficiency of 80% is 122.4 mA cm^{-2} through the linear interpolation of experimental data, while the current density of the ICRFB at energy efficiency of 81% is 92.6 mA cm^{-2} (extra 1% offsets the loss of rebalancing process). The advanced VRFB based on mixed acids delivers better stability and wider operating temperature window [32,36]. Hence, the heat exchanger is unnecessary and not considered for the VRFB. The base case of the 1 MW–8 h energy storage system is analyzed for the two types of RFBs. The input data are list in Table 2.

Table 2
Parameters of the VRFB and ICRFB for the base case of 1 MW–8 h energy storage system.

Energy storage system	ICRFB	VRFB
System power output, kW	1000	1000
Discharge time, h	8	8
Theoretic voltage@50%SOC, V	1	1.36
Average discharge voltage, V	0.94	1.25
Single cell energy efficiency	0.81	0.8
Power of system loss, kW	40	40
Utilization of electrolyte	0.7	0.7
Maximum flow rate, mL/min/cm^2	2	2
Current density, mA/cm^2	92.6	122.4

Table 3
Component cost of redox flow batteries.

Component	Cost	Reference
Membrane, \$/m^2	500	[30]
Bipolar plate, \$/m^2	55	[30]
Graphite felt, \$/m^2	70	[30]
PVC frame, \$/m^2	16.56	[30]
Ferrochromium (Cr content), \$/kg	2.362	[35]
V_2O_5, \$/kg	14.31	[35]
Gaskets, bolts, end plates, \$/m^2	14	[30]
Stack manufactory	10% of stack material	[19]
Heat exchanger, \$/kW	84	[30]
PCS, \$/kW	210	[30]
Thermal insulation material, \$/m^2	15	[34]
Tank, \$/gallon	0.29	[30]
Pump, \$/GPM	18	[30]
Rebalance cell, \$/kW	8.27	one rebalance cell for a 100-cell stack

4. Results and discussion

4.1. Charge–discharge performance of VRFB and ICRFB

The two RFBs are tested at their respective typical operating temperatures. The VRFB generally operates under room temperature, and the cooling system is necessary to avoid precipitation of

Table 1
Efficiencies of the VRFB and ICRFB at the various current densities.

Current density/mA/cm2	VRFB CE	VRFB VE	VRFB EE	ICRFB CE	ICRFB VE	ICRFB EE
40	95.3	93.7	89.4	90.5	93.3	84.4
80	97.3	87.8	85.4	94.6	87.0	82.2
120	97.8	82.1	80.3	96.8	81.0	78.4
160	98.2	76.6	75.2	97.7	75.7	73.9

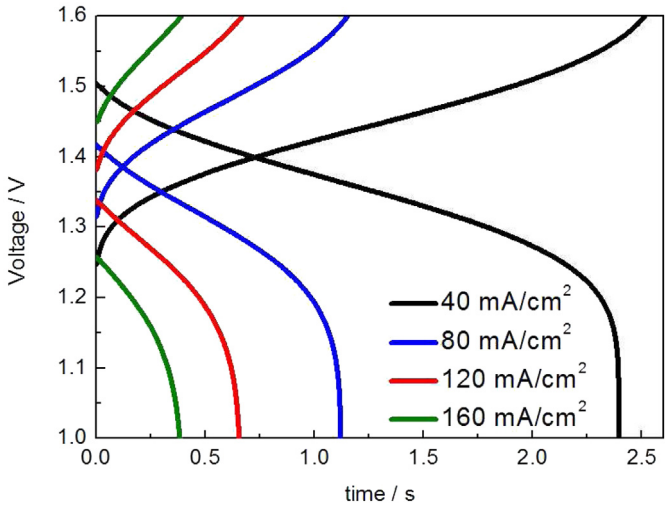

Fig. 2. Charge–discharge curves of the VRFB.

V(V) species at higher temperatures (>40 °C) [37]. In comparison, the ICRFB typically operates at a temperature of 65 °C to avoid the issue of chromium aging with the thermal management system [10]. The charge–discharge curves of the VRFB and the ICRFB are shown in Fig. 2 and Fig. 3, respectively. The efficiencies (CE, VE, EE) of two RFBs are listed in Table 1. The voltage efficiencies of the ICRFB are comparable with the VRFB at various current densities. At a current density of 40 mA cm^{-2}, the voltage efficiencies of the VRFB and ICRFB are 93.7% and 93.3% respectively, which indicates that the two RFBs both have good electrochemical kinetics. The coulombic efficiencies of the ICRFB are lower than that of the VRFB mainly due to a higher crossover rate and higher side reaction rate at the higher operating temperature (65 °C). With an increased current density, the coulombic efficiencies of both batteries also increase. This is because the charge–discharge time decreases with the current density, resulting in a decreased crossover amount of active species and thus higher coulombic efficiency. The energy efficiencies of the VRFB and ICRFB at a current density of 120 mA cm^{-2} are able to reach 80.3% and 78.4%, respectively. It is shown that the charge–discharge performances of two RFBs are very similar at high current densities.

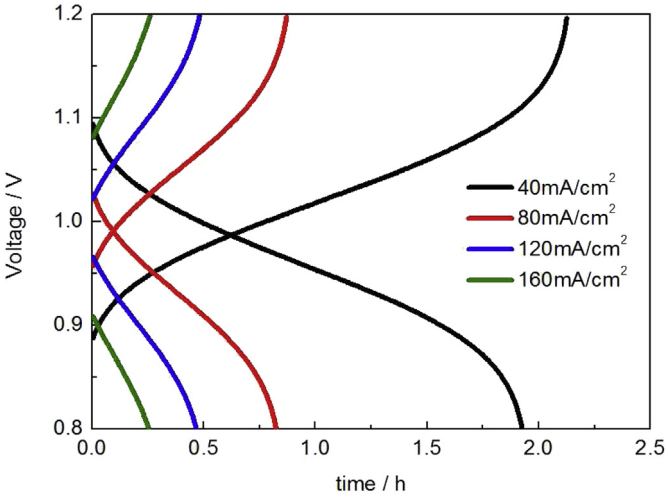

Fig. 3. Charge–discharge curves of the ICRFB.

4.2. Cycle performance of VRFB and ICRFB

The efficiencies (CE, VE, EE) of the VRFB and ICRFB versus the cycle number are shown in Fig. 4 and Fig. 5. During 30 cycles, the coulombic efficiency and the voltage efficiency of the two batteries are both relatively stable. The capacity decay versus the cycle number is shown in Fig. 6. The capacity decay rate of the VRFB is around 0.3% capacity per cycle, while it is 1.2% for the ICRFB. A higher decay rate for ICRFB is mainly attributed to higher rates of hydrogen evolution and crossover due to ICRFB running at a higher operating temperature. During the extended cycles, hydrogen evolution at the negative electrode causes accumulation of ferric ions at the positive electrolyte, which leads to an imbalance of SOC between the positive and negative electrolytes, and induces capacity decay. To avoid capacity decay, the practical ICRFB energy storage system is typically equipped with rebalancing cells [9,38,39]. An iron–chlorine rebalance cell was proposed and demonstrated excellent stability during operation over a period of one year [9]. Excess ferric chloride was electrolyzed to ferrous chloride and chlorine gas, and then chlorine gas reacted with evolved hydrogen to rebalance the SOC. The capacity decay rate of the ICRFB was reported to reduce from 2% to 0.3% per cycle with the addition of a rebalancing cell [38].

4.3. Capital cost of VRFB and ICRFB

The capital cost breakdown of the two RFBs is shown in Fig. 7 for the base case of the 1 MW–8 h energy storage system. The VRFB electrolyte costs \$122 kWh^{-1}, accounting for 53% of the system capital cost due to the high cost of vanadium materials. In comparison, the cost of ICRFB electrolyte is estimated at \$17 kWh^{-1}, only accounting for 9% of the ICRFB capital cost. Iron and chromium are low-cost active materials, providing a huge potential for the ICRFB to reduce the system cost. The RFB capital cost involving the various application scenarios of discharge duration is shown in Fig. 8. A longer duration indicates larger capacity of storage energy as the power remains the same. The capital cost of the present ICRFB is lower than that of the present VRFB for the application scenarios with discharge duration larger than 5.5 h. For the given battery, a higher current density indicates a higher power density, which reduces the capital cost of cell stacks. The improved VRFB and ICRFB in Fig. 8 are assumed to double the current density of

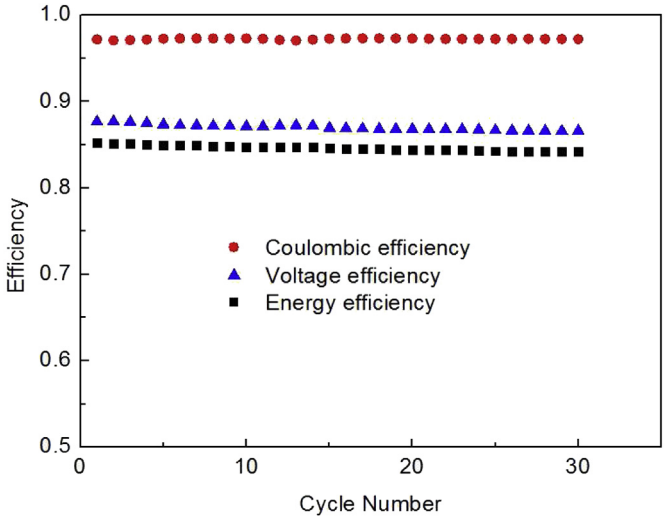

Fig. 4. Efficiency of the VRFB versus the cycle number.

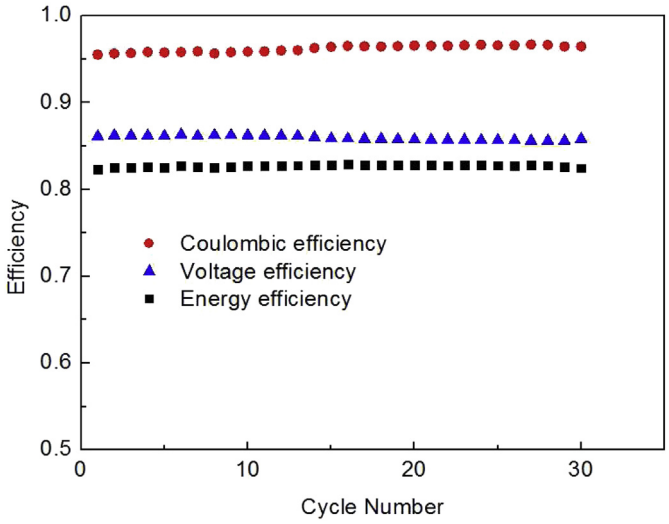

Fig. 5. Efficiency of the ICRFB versus the cycle number.

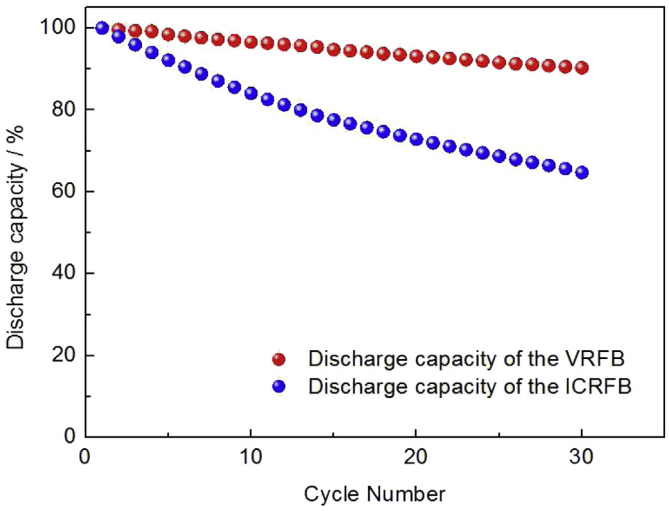

Fig. 6. Discharge capacity of the VRFB and ICRFB versus the cycle number.

their present versions with energy efficiency kept unchanged. The capital cost of the ICRFB decreases significantly with improved performance, while capital cost reduction of the VRFB is relatively limited as the vanadium materials sets a high floor on the capital cost. The performance of the ICRFB is expected to improve with further extensive research, and potentially achieve a cost-effective energy storage system. It is worth noting that cheap hydrocarbon membranes can be used in the ICRFB system [11], which will further reduce the capital cost of ICRFBs.

5. Conclusions

For large-scale energy storage systems, the energy efficiency, cycle life, and capital cost are major considerations for commercialization. A comprehensive comparison, including the charge–discharge tests, cycle tests and the capital cost analyses, was carried out for the VRFB and ICRFB. The ICRFB exhibits similar energy efficiency with the VRFB at high current densities. The energy efficiency of 80.3% and 78.4% can be achieved for the VRFB and the ICRFB at 120 mA cm^{-2}, respectively. During the cycle test, efficiencies of two RFBs are both stable. The capacity decay rate of the

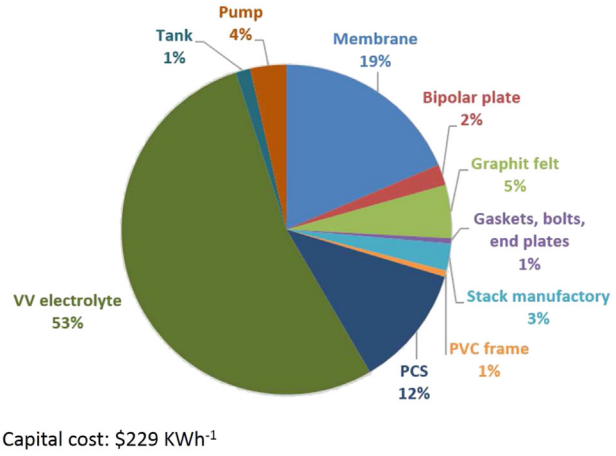

(a)

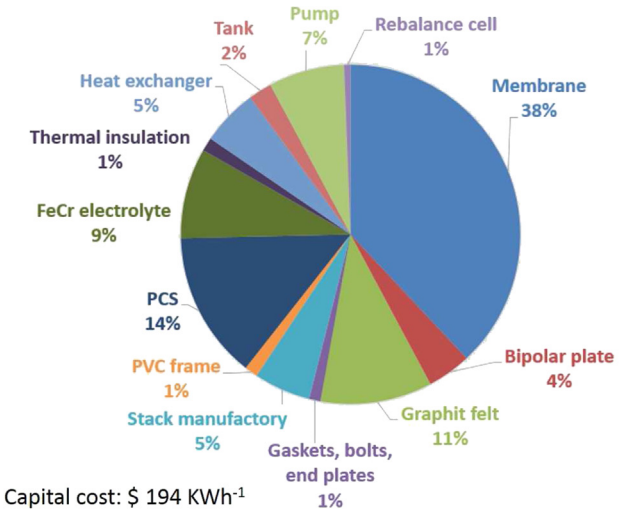

(b)

Fig. 7. Capital cost breakdown of the base case for (a) the VRFB and (b) ICRFB.

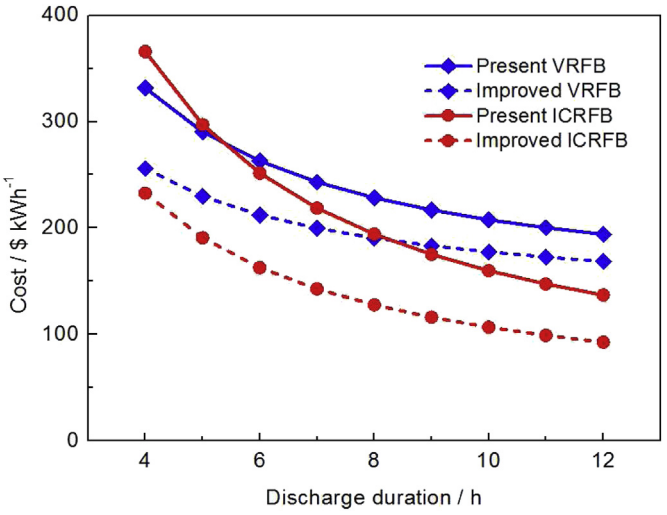

Fig. 8. Capital cost of the VRFB and ICRFB versus the discharge duration.

ICRFB is 1.2% per cycle, higher than 0.3% per cycle of the VRFB, due to the higher crossover rate and higher side reaction rate caused by higher operating temperatures. The capital cost analysis indicates that the cost of the ICRFB can be significantly lowered if the current density is increased or if the discharge duration is lengthened.

Acknowledgments

The work described in this paper was fully supported by a grant from the Research Grants Council of the Hong Kong Special Administrative Region, China (Project No. 16213414).

References

[1] C.P. De Leon, A. Frías-Ferrer, J. González-García, D. Szánto, F.C. Walsh, Redox flow cells for energy conversion, J. Power Sources 160 (2006) 716–732.
[2] W. Wang, Q. Luo, B. Li, X. Wei, L. Li, Z. Yang, Recent progress in redox flow battery research and development, Adv. Funct. Mater. 23 (2013) 970–986.
[3] Z. Yang, J. Zhang, M.C. Kintner-Meyer, X. Lu, D. Choi, J.P. Lemmon, J. Liu, Electrochemical energy storage for green grid, Chem. Rev. 111 (2011) 3577–3613.
[4] L.H. Thaller, Electrically Rechargeable Redox Flow Cells, NASA TM X-71540, Lewis Research Centre, 1974.
[5] D.S. Cheng, E. Hollax, The influence of thallium on the redox reaction Cr^{3+}/Cr^{2+}, J. Electrochem. Soc. 132 (1985) 269–273.
[6] E. Hollax, D.S. Cheng, The influence of oxidative pretreatment of graphite electrodes on the catalysis of the Cr^{3+}/Cr^{2+} and Fe^{3+}/Fe^{2+} redox reactions, Carbon 23 (1985) 655–664.
[7] D.A. Johnson, M.A. Reid, Chemical and electrochemical behavior of the Cr(III)/Cr(II) half-cell in the iron-chromium redox energy storage system, J. Electrochem. Soc. 132 (1985) 1058–1062.
[8] C. Wu, D. Scherson, E. Calvo, E. Yeager, M. Reid, A bismuth-based electrocatalyst for the chromous-chromic couple in acid electrolytes, J. Electrochem. Soc. 133 (1986) 2109–2112.
[9] R.F. Gahn, N.H. Hagedorn, J.A. Johnson, Cycling Performance of the Iron-chromium Redox Energy Storage System, NASA TM-87034, Lewis Research Centre, 1985.
[10] R.F. Gahn, N.H. Hagedorn, J.S. Ling, Single Cell Performance Studies on the Fe/Cr Redox Energy Storage System Using Mixed Reactant Solutions at Elevated Temperature, NASA TM-83385, Lewis Research Centre, 1983.
[11] W. Wang, S. Kim, B. Chen, Z. Nie, J. Zhang, G.-G. Xia, L. Li, Z. Yang, A new redox flow battery using Fe/V redox couples in chloride supporting electrolyte, Energy Environ. Sci. 4 (2011) 4068–4073.
[12] Q. Luo, L. Li, W. Wang, Z. Nie, X. Wei, B. Li, B. Chen, Z. Yang, V. Sprenkle, Capacity decay and remediation of nafion-based all-vanadium redox flow batteries, ChemSusChem 6 (2013) 268–274.
[13] G. Codina, A. Aldaz, Scale-up studies of an Fe/Cr redox flow battery based on shunt current analysis, J. Appl. Electrochem. 22 (1992) 668–674.
[14] G. Codina, J. Perez, M. Lopez-Atalaya, J. Vasquez, A. Aldaz, Development of a 0.1 kw power accumulation pilot plant based on an Fe/Cr redox flow battery part I. Considerations on flow-distribution design, J. Power Sources 48 (1994) 293–302.
[15] V. Jalan, B. Morriseau, L. Swette, Optimization and Fabrication of Porous Carbon Electrodes for Fe/Cr Redox Flow Cells, NASA-CR-167921, Giner, Inc., 1982.
[16] Enervault corporation. Available from: Http://enervault.com/. (accessed 11.07.15.).
[17] M. Rychcik, M. Skyllas-Kazacos, Characteristics of a new all-vanadium redox flow battery, J. Power Sources 22 (1988) 59–67.
[18] C. Ding, H. Zhang, X. Li, T. Liu, F. Xing, Vanadium flow battery for energy storage: prospects and challenges, J. Phys. Chem. Lett. 4 (2013) 1281–1294.
[19] H. Kamath, S. Rajagopalan, M. Zwillenberg, Vanadium Redox Flow Batteries: an In-depth Analysis, EPRI 1014836, Electric Power Research Institute, Palo Alto, CA, 2007.
[20] K.J. Kim, M.-S. Park, Y.-J. Kim, J.H. Kim, S.X. Dou, M. Skyllas-Kazacos, A technology review of electrodes and reaction mechanisms in vanadium redox flow batteries, J. Mater. Chem. A 3 (2015) 16913–16933.
[21] E. Sum, M. Skyllas-Kazacos, A study of the V(II)/V(III) redox couple for redox flow cell applications, J. Power Sources 15 (1985) 179–190.
[22] D. Aaron, Q. Liu, Z. Tang, G. Grim, A. Papandrew, A. Turhan, T. Zawodzinski, M. Mench, Dramatic performance gains in vanadium redox flow batteries through modified cell architecture, J. Power Sources 206 (2012) 450–453.
[23] B. Li, M. Gu, Z. Nie, Y. Shao, Q. Luo, X. Wei, X. Li, J. Xiao, C. Wang, V. Sprenkle, Bismuth nanoparticle decorating graphite felt as a high-performance electrode for an all-vanadium redox flow battery, Nano Lett. 13 (2013) 1330–1335.
[24] Q. Liu, G. Grim, A. Papandrew, A. Turhan, T.A. Zawodzinski, M.M. Mench, High performance vanadium redox flow batteries with optimized electrode configuration and membrane selection, J. Electrochem. Soc. 159 (2012) A1246–A1252.
[25] M.L. Perry, R.M. Darling, R. Zaffou, High power density redox flow battery cells, ECS Trans. 53 (2013) 7–16.
[26] X. Zhou, T. Zhao, L. An, L. Wei, C. Zhang, The use of polybenzimidazole membranes in vanadium redox flow batteries leading to increased coulombic efficiency and cycling performance, Electrochim. Acta 153 (2015) 492–498.
[27] D. Chen, M.A. Hickner, E. Agar, E.C. Kumbur, Selective anion exchange membranes for high coulombic efficiency vanadium redox flow batteries, Electrochem. Commun. 26 (2013) 37–40.
[28] X. Zhou, T. Zhao, L. An, Y. Zeng, X. Yan, A vanadium redox flow battery model incorporating the effect of ion concentrations on ion mobility, Appl. Energy 158 (2015) 157–166.
[29] K. Knehr, E. Agar, C. Dennison, A. Kalidindi, E. Kumbur, A transient vanadium flow battery model incorporating vanadium crossover and water transport through the membrane, J. Electrochem. Soc. 159 (2012) A1446–A1459.
[30] V. Viswanathan, A. Crawford, D. Stephenson, S. Kim, W. Wang, B. Li, G. Coffey, E. Thomsen, G. Graff, P. Balducci, Cost and performance model for redox flow batteries, J. Power Sources 247 (2014) 1040–1051.
[31] C. Wadia, P. Albertus, V. Srinivasan, Resource constraints on the battery energy storage potential for grid and transportation applications, J. Power Sources 196 (2011) 1593–1598.
[32] S. Kim, E. Thomsen, G. Xia, Z. Nie, J. Bao, K. Recknagle, W. Wang, V. Viswanathan, Q. Luo, X. Wei, 1 kw/1 kwh advanced vanadium redox flow battery utilizing mixed acid electrolytes, J. Power Sources 237 (2013) 300–309.
[33] R.M. Darling, K.G. Gallagher, J.A. Kowalski, S. Ha, F.R. Brushett, Pathways to low-cost electrochemical energy storage: a comparison of aqueous and nonaqueous flow batteries, Energy Environ. Sci. 7 (2014) 3459–3477.
[34] E. Cuce, P.M. Cuce, C.J. Wood, S.B. Riffat, Toward aerogel based thermal superinsulation in buildings: a comprehensive review, J. Renew. Sustain. Energy 34 (2014) 273–299.
[35] U.S. Geological survey. Commodity statistics and information. Available from: Http://minerals.usgs.gov/minerals/pubs/commodity/. (accessed 13.07.15.).
[36] L. Li, S. Kim, W. Wang, M. Vijayakumar, Z. Nie, B. Chen, J. Zhang, G. Xia, J. Hu, G. Graff, A stable vanadium redox-flow battery with high energy density for large-scale energy storage, Adv. Energy Mater. 1 (2011) 394–400.
[37] M. Vijayakumar, L. Li, G. Graff, J. Liu, H. Zhang, Z. Yang, J.Z. Hu, Towards understanding the poor thermal stability of V^{5+} electrolyte solution in vanadium redox flow batteries, J. Power Sources 196 (2011) 3669–3672.
[38] L.H. Thaller, Recent Advances in Redox Flow Cell Storage Systems, NASA TM-79186, Lewis Research Centre, 1979.
[39] A.H. Whitehead, M. Harrer, Investigation of a method to hinder charge imbalance in the vanadium redox flow battery, J. Power Sources 230 (2013) 271–276.

Nomenclature

A: electrode area, m^2
i_d: discharge current density, A m^{-2}
$\overline{V}_d$: average discharge voltage, V
V: electrolyte volume, m^3
P_{rated}: Rated discharge power, W
P_{loss}: Power of system loss including pump losses, shunt current loss and so on, W
t_d: discharge time, s
x: concentration of active species, mol m^{-3}
ε: SOC utilization range
$C_{P,M}$: manufacturing cost of the power part (cell stacks), \$ W^{-1}
$C_{E,M}$: manufacturing cost of energy part (electrolyte), \$ W^{-1}
Q_i: cost of materials, \$ kg^{-1}
Q_t: cost of tank per volume, \$ m^{-3}
M_i: molar mass of active species, kg mol^{-1}
S_i: stoichiometric number